Propagation and breathing of matter–wave-packet trains

Wenhua Hai,[1,*] Chaohong Lee,[2] and Guishu Chong[1]
[1]*Department of Physics, Hunan Normal University, Changsha 410081, China*
[2]*Max-Planck-Institut für Physik komplexer Systeme, Nöthnitzer Straße 38, D-01187 Dresden, Germany*
(Received 9 June 2004; published 24 November 2004)

We find a set of different orthonormalized states of a nonstationary harmonic oscillator and use them to expand the solution of the Gross-Pitaevskii equation with harmonic potential. The expansion series describes wave-packet trains of a Bose-Einstein condensate, which may be induced initially by the modulational instability. The center of any wave-packet train oscillates like a classical harmonic oscillator of frequency ω. The width and height of the wave packet and the distance between two wave packets change simultaneously like an array of breathers with frequency 2ω. We demonstrate analytically and numerically that for a set of suitable parameters the wave-packet trains can be more exactly fitted to the matter-wave soliton trains observed by Strecker *et al.* and reported in Nature (London) **417**, 150 (2002).

DOI: 10.1103/PhysRevA.70.053621 PACS number(s): 03.75.Lm, 03.75.Kk, 03.65.Ge, 05.30.Jp

I. INTRODUCTION

Recently, a kind of important nonlinear phenomenon, the soliton behavior in a Bose-Einstein condensate (BEC), has been experimentally observed and theoretically studied [1–11]. In Strecker's experiment, the bright soliton trains were formed by magnetically tuning the atom-atom interaction in a stable BEC from repulsive to attractive, then were set to propagate and breathe in the potential for many oscillatory cycles without spreading [1]. In the theoretical works, Carr and Brand [4] and Salasnich *et al.* [5] investigated the formation and evolution of the matter-wave bright solitons in a BEC governed by a time-dependent Gross-Pitaevskii equation (GPE) and pointed out that the solitons are induced by the modulational instability in a BEC. By attributing the formation of soliton trains to the quantum phase fluctuations, Al Khawaja *et al.* gave a similar result from a GPE with the harmonic confinement [6].

Here we are interested in the propagation and breathing of the Strecker's soliton trains. We know well that the solitons with oscillating mass center have never been found yet in a standard nonlinear Schrödinger equation without the harmonic potential. However, the wave packet in a coherent state of a harmonic oscillator can oscillate their centers [12,13]. Therefore, after the soliton trains are initially produced, the harmonic potential may play a leading role for dominating their motions and this leading role can be shown by using some interesting coherent states of the harmonic oscillator to expand the solution of the GPE.

In previous work, we investigated another kind of nonlinear phenomenon, the chaotic behavior of the BEC in the time-dependent double-well potentials [14–17]. In this paper we consider a BEC consisting of N identical Bose atoms and being transferred into a cigar-shaped harmonic trap. Let the transverse frequencies ω_r be much greater than the axial frequencies ω_x; the dynamics of the system is governed by the quasi-one-dimensional (quasi-1D) GPE [6,18],

$$i\hbar\frac{\partial\psi}{\partial t}=-\frac{\hbar^2}{2m}\frac{\partial^2\psi}{\partial x^2}+\left[\frac{1}{2}m\omega_x^2x^2+g_{1d}|\psi|^2\right]\psi, \tag{1}$$

where we have assumed the transverse wave function is in the ground state of a harmonic oscillator such that the quasi-1D interaction intensity g_{1d} related to the s-wave scattering length a_s, atomic mass m, and number of condensed atoms N is [19] $g_{1d}=Nm\omega_r g_0/(2\pi\hbar)=2N\hbar\omega_r a_s$ for the normalized wave function ψ. The norm $|\psi|^2$ is the probability density and $N|\psi|^2$ the density of atomic number. Setting $l_r=\sqrt{\hbar/(m\omega_r)}$, $l_x=\sqrt{\hbar/(m\omega_x)}$, and writing E_{kin} and E_{int} as the kinetic energy and mean-field interaction energy of the BEC, the relationship $E_{int}/E_{kin}\sim N|a_s|/(l_r^2l_x)^{1/3}$ expresses the importance of the atom-atom interaction compared to the kinetic energy [18]. For a small particle number or short s-wave scattering length [1,2], the interaction term is relatively weak. For example, in the experimental parameters of Strecker *et al.*'s bright solitons [1,6], the parameters ω_x, ω_r and $|a_s|$ are in order of 10 s^{-1}, 10^2 s^{-1}, and 10^{-10} m, respectively. Although the number of the initially condensed atoms is approximately 3×10^5, "most of the atoms from the collapsing condensate are lost, while only a small fraction remain as solitons" [1]. So the previous work took the number of condensed atoms as $N=10^4$ to fit the bright solitons [6]. Using these parameters and the mass of the ^{7}Li atom to calculate l_x and l_r, we get the ratio of E_{int} to E_{kin} as $N|a_s|/(l_r^2l_x)^{1/3}<10^{-1}$. Compared to the interaction intensity $g_{1d}=2N\hbar\omega_r a_s$ with parameters $N\sim10^5$, $|a_s|\sim10^{-9}$ m of the common case [18], the interaction intensity in Strecker's experiment is very weak such that the harmonic potential may play an important role. In such a case, using a set of orthonormalized harmonic-oscillator states to expand the solution of GPE can give good converged results for the nonlinear system. Particularly, if the harmonic-oscillator states describe some wave-packet trains of the linear system [12,20], the corresponding series solution can describe the soliton trains of the nonlinear system. We shall report a set of different orthonormalized coherent states of a nonstationary

*Corresponding author.
Electronic address: adcve@public.cs.hn.cn

harmonic oscillator and use them to expand the solution of GPE with the harmonic potential and weak atom-atom interaction. By using them we demonstrate that, analytically and numerically, the wave-packet trains governed by the series solution can be more exactly fitted to Strecker's matter-wave soliton trains.

II. ORTHONORMALIZED STATES OF A HARMONIC OSCILLATOR

In order to construct the Strecker's soliton solution, we first seek the coherent states (wave-packet solutions) of a nonstationary harmonic oscillator. We adopt the natural unit with $m=\hbar=\omega_x=1$ to yield the time-dependent Schrödinger equation

$$i\frac{\partial \psi_n^{(0)}}{\partial t} = -\frac{1}{2}\frac{\partial^2\psi_n^{(0)}}{\partial x^2} + \frac{1}{2}x^2\psi_n^{(0)}, \tag{2}$$

where t and x are in units of ω_x^{-1} and l_x, respectively. It is well known that this equation has not only the stationary solutions, but also the nonstationary solutions, say the coherent-state solution. Let the solution of Eq. (2) be in the form

$$\psi_n^{(0)} = a_n(t)H_n(\xi)e^{[b(t)x-c(t)x^2-f^2(t)/2]},$$

$$\xi = e(t)x - f(t), \tag{3}$$

with $a_n(t)$, $b(t)$, $c(t)$ being the complex functions of time and $e(t)$, $f(t)$ the real functions, and $H_n(\xi)$ the Hermitian polynomial of variable ξ. The direct calculations from Eq. (3) give

$$i\frac{\partial \psi_n^{(0)}}{\partial t} = ia_n\left(\frac{\dot{a}_n}{a_n}H_n + (\dot{e}x-\dot{f})\frac{\partial H_n}{\partial \xi} + (\dot{b}x - f\dot{f} - \dot{c}x^2)H_n\right)e^{[b(t)x-c(t)x^2-f^2(t)/2]},$$

$$\frac{\partial^2\psi_n^{(0)}}{\partial x^2} = a_n\left(e^2\frac{\partial^2 H_n}{\partial \xi^2} + (2b-4cx)e\frac{\partial H_n}{\partial \xi} + (b^2-2c-4bcx+4c^2x^2)H_n\right)e^{[b(t)x-c(t)x^2-f^2(t)/2]}.$$

Applying the two equations to Eq. (2) leads to the equation

$$e^2\frac{\partial^2 H_n}{\partial \xi^2} + 2(be - i\dot{f} + i\dot{e}x - 2cex)\frac{\partial H_n}{\partial \xi} + 2\left[i\frac{\dot{a}_n}{a_n} - if\dot{f} + \frac{b^2}{2} - c - (i\dot{b}-2bc)x + \left(2c^2 - i\dot{c} - \frac{1}{2}\right)x^2\right]H_n = 0. \tag{4}$$

Notice that the Hermitian polynomial must obey the Hermitian equation $\partial^2 H_n/\partial\xi^2 - 2\xi\partial H_n/\partial\xi + 2nH_n = 0$. Comparing this with Eq. (4), we arrive at

$$i\dot{c} = 2c^2 - 1/2, \quad i\dot{b} = 2bc, \quad i\dot{e} = 2ce - e^3,$$

$$i\dot{f} = be - e^2 f, \quad i\dot{a}_n/a_n = if\dot{f} - b^2/2 + c + ne^2. \tag{5}$$

These equations are similar to Eq. (4) of Ref. [12], where the first equation contains a periodic driven term. Without the periodic driven in Eq. (5) we can easily derive its exact solution as follows. The first of Eq. (5) is a complex Riccati equation, which can be transformed into a complex equation of a classical harmonic oscillator,

$$\ddot{\varphi} = -\varphi, \tag{6}$$

through the function transformation $c=\dot{\varphi}/(2i\varphi)$. The general solution of Eq. (6) is well known:

$$\varphi = A\cos(t+\alpha) + iB\cos(t+\beta) = \rho(x,t)\exp[i\theta(x,t)], \tag{7}$$

where A, B, α, and β are arbitrary constants adjusted by the initial conditions of the classical harmonic oscillator, the real functions $\rho(x,t)$ and $\theta(x,t)$ read as

$$\rho = \sqrt{A^2\cos^2(t+\alpha) + B^2\cos^2(t+\beta)},$$

$$\theta = \arctan\frac{B\cos(t+\beta)}{A\cos(t+\alpha)}. \tag{8}$$

Given Eq. (7), the transformation between φ and c can be written as

$$c = \frac{\dot{\varphi}}{2i\varphi} = \frac{1}{2}\dot{\theta} - i\frac{\dot{\rho}}{2\rho}. \tag{9}$$

Substituting Eq. (7) into Eq. (6) yields the equations of the amplitude and phase as

$$\ddot{\theta} = -2\dot{\theta}\dot{\rho}/\rho, \quad \ddot{\rho} = \rho\dot{\theta}^2 - \rho \tag{10}$$

with the first integrations

$$c_0 = \rho^2\dot{\theta} = AB\sin(\alpha-\beta),$$

$$c_1 = (\dot{\rho}^2 + c_0^2/\rho^2 + \rho^2)/2. \tag{11}$$

Combining Eqs. (9) and (8) with Eq. (5) and applying the relation (11), we easily obtain the functions

$$b = b_0\frac{\exp(-i\theta)}{\rho}, \quad e = \frac{\sqrt{c_0}}{\rho} = \sqrt{\dot{\theta}}, \quad f = \frac{b_0}{\sqrt{c_0}}\cos\theta,$$

$$a_n = \frac{A_n}{\sqrt{\rho}}\exp\left\{-i\left[\left(\frac{1}{2}+n\right)\theta - \frac{b_0^2}{4c_0}\sin 2\theta\right]\right\} \tag{12}$$

in terms of the real functions $\rho(t)$ and $\theta(t)$. Here b_0 is an arbitrary constant and A_n the normalization constant. Inserting Eqs. (9) and (12) into Eq. (3) leads to the exact solution $\psi_n^{(0)}(x,t)$, then the normalization condition $\int|\psi_n^{(0)}|^2 dx = A_n^2\sqrt{c_0^{-1}}\int H_n^2(\xi)\exp(-\xi^2)d\xi = A_n^2\sqrt{\pi c_0^{-1}}2^n n! = 1$ gives the normalization constant $A_n = [\sqrt{c_0}/(\sqrt{\pi}2^n n!)]^{1/2}$, where the wave function $\psi_n^{(0)}$ has been normalized in unit $l_x^{-1/2}$. Applying Eqs. (9)–(12) and the normalization constant to Eq. (3), we get the orthonormalized exact solution,

$$\psi_n^{(0)} = R_n^{(0)}\exp[i\Theta^{(0)}(x,t) - in\theta(t)], \quad n=0,1,2,\ldots,$$

$$R_n^{(0)} = \left[\frac{\sqrt{c_0}}{\sqrt{\pi}2^n n!\rho(t)}\right]^{1/2} H_n(\xi)\exp\left[-\frac{1}{2}\xi^2\right],$$

$$\xi = \frac{\sqrt{c_0}x}{\rho(t)} - \frac{b_0}{\sqrt{c_0}}\cos\theta(t),$$

$$\Theta^{(0)} = \frac{\dot{\rho}(t)x^2}{2\rho(t)} - \frac{b_0 x}{\rho(t)}\sin\theta(t) + \frac{b_0^2}{4c_0}\sin[2\theta(t)] - \frac{1}{2}\theta(t). \tag{13}$$

Obviously, the solution (13) is not a energy eigenstate, but denotes a different kind of coherent state [12]. In the mathematical point of view, it is a complete solution with the independent constants A, B, α, β, b_0, and c_0. By adjusting these constants, we can use the complete solution to describe some different quantum states. It is easy to prove the solution (13) obeying the orthonormalization condition. According to the property of the Hermitian polynomial, the probability density $(R_n^{(0)})^2$ describes the wave-packet trains consisting of $n+1$ packets, since it is proportional to the function $[H_n(\xi)]^2$. By using Eqs. (13) and (8), from $\xi=0$ we have the orbit of the center of wave-packet trains,

$$x_c = \frac{b_0}{c_0}\rho(t)\cos\theta(t) = \frac{b_0}{c_0}A\cos(t+\alpha), \tag{14}$$

which is proportional to the real part of the complex solution φ and describes the motion of a classical harmonic oscillator of unit mass with amplitude Ab_0/c_0, frequency ω_x, and initial phase α.

Now we calculate the average energy under the state (13). Employing the Dirac's symbols, ket, and bra, from Eq. (3) and the quantum-mechanical definition of average energy in state $\psi_n^{(0)}$, we perform the calculation

$$E_n = \langle\psi_n^{(0)}|i\frac{\partial}{\partial t}\psi_n^{(0)}\rangle = i\langle\psi_n^{(0)}|\frac{\dot{a}_n}{a_n} + (\dot{e}x - \dot{f})\frac{1}{H_n}\frac{\partial H_n}{\partial \xi} - (f\dot{f} - \dot{b}x + \dot{c}x^2)|\psi_n^{(0)}\rangle. \tag{15}$$

Noticing the orthonormalization condition $\langle\psi_n^{(0)}|\psi_{n'}^{(0)}\rangle = \delta_{nn'}$ and the formulas

$$\xi = e(t)x - f(t), \quad \xi\psi_n^{(0)} = \sqrt{n/2}\,\psi_{n-1}^{(0)} + \sqrt{(n+1)/2}\,\psi_{n+1}^{(0)},$$

$$2\xi^2\psi_n^{(0)} = \sqrt{n(n-1)}\,\psi_{n-2}^{(0)} + (2n+1)\psi_n^{(0)} + \sqrt{(n+1)(n+2)}\,\psi_{n+2}^{(0)},$$

$$\frac{1}{H_n}\frac{\partial H_n}{\partial \xi}\psi_n^{(0)} = 2n\frac{H_{n-1}}{H_n}\psi_n^{(0)} = \sqrt{2n}\,\psi_{n-1}^{(0)},$$

we continue to compute the average energy,

$$E_n = i\left(\frac{\dot{a}_n}{a_n} - f\dot{f}\right) + i\langle\psi_n^{(0)}|\sqrt{2n}\dot{e}\xi/e|\psi_{n-1}^{(0)}\rangle + i\langle\psi_n^{(0)}|\dot{b}x - \dot{c}x^2|\psi_n^{(0)}\rangle$$
$$= i\left\{\frac{\dot{a}_n}{a_n} - f\dot{f} + n\frac{\dot{e}}{e} - \frac{\dot{c}}{e^2}\left[f^2 + \left(\frac{1}{2}+n\right)\right]\right\} + i\frac{\dot{b}f}{e}.$$

Applying Eqs. (5) to the above equation and noticing Eqs. (9), (11), and (12) result in

$$E_n = (2n+1)c - \frac{b^2}{2} - \left(2c^2 - \frac{1}{2}\right)\left[f^2 + \left(\frac{1}{2}+n\right)\right]\frac{1}{e^2} + 2bc\frac{f}{e}$$
$$= \left(\frac{1}{2}+n\right)\frac{c_1}{c_0} + \frac{b_0^2}{c_0}c_2, \quad n = 0,1,2,\ldots. \tag{16}$$

Here c_2 is another integration constant,

$$c_2 = \frac{A^2 c_1}{(A^2+B^2)c_0}, \tag{17}$$

and $b_0^2 c_2/c_0 = b_0^2 A^2 c_1/[c_0^2(A^2+B^2)]$ is proportional to the square of the amplitude of Eq. (14) or the energy of the classical oscillator. For the given constants b_0 and c_i, $i=0,1,2$, Eq. (16) exhibits that the average energy only depends on the quantum number n. It is quite interesting that the average energy (16) is proportional to both the quantum level and the classical energies of the harmonic oscillators dominated by Eqs. (6) and (14). A higher quantum level is associated with a wave-packet train with more packets, namely the number of packets is $n+1$ for the wave function $\psi_n^{(0)}$. We shall use the wave-packet solutions of Eq. (13) as a set of basic vectors to expand the solution of the nonlinear GPE and employ the latter to fit Strecker's matter-wave soliton trains in the following section.

III. FITTING TO STRECKER'S MATTER-WAVE SOLITON TRAINS

Given the orthonormalized solution $\psi_n^{(0)}(x,t)$, we apply them to expand the solution of the GPE as

$$\psi(x,t) = \sum_{n=0}^{\infty} C_n(t)\psi_n^{(0)}(x,t) = e^{i\Theta^{(0)}(x,t)}\sum_{n=0}^{\infty} C_n(t)R_n^{(0)}(\xi,t)e^{-in\theta(t)}, \tag{18}$$

with $C_n(t)$ being the expansion coefficient. Substituting such ψ into Eq. (1) yields the equation of the expansion coefficients as

$$\sum_{n=0}^{\infty} i\dot{C}_n(t)\psi_n^{(0)}(x,t) = g_{1d}|\psi(x,t)|^2\psi(x,t). \tag{19}$$

Noticing Eq. (18) and the orthonormalization condition of Eq. (13), we simplify Eq. (19) to

$$i\dot{C}_n(t) = g_{1d}\int_{-\infty}^{\infty}|\psi|^2\psi\psi_n^{*(0)}dx = g_{1d}\sum_{ijk} I_{ijk}^n(t)C_i^*(t)C_j(t)C_k(t) \tag{20}$$

for $n=0,1,2,\ldots$, where I_{ijk}^n are defined by [21]

$$I_{ijk}^n(t) = \int_{-\infty}^{\infty}\psi_i^{*(0)}\psi_j^{(0)}\psi_k^{(0)}\psi_n^{*(0)}dx. \tag{21}$$

We have known that the probability density $(R_n^{(0)})^2$ describes the wave-packet trains consisting of $n+1$ packets of the linear harmonic oscillator. The corresponding wave-packet trains of the nonlinear system (1) is described by the norm of ψ in Eq. (18), that is,

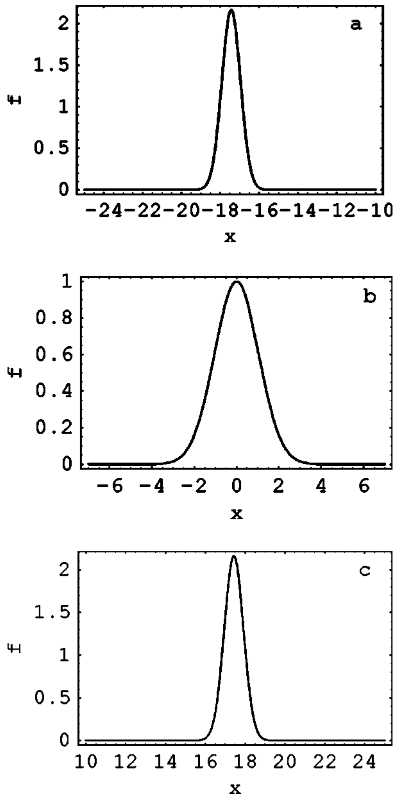

FIG. 1. The function $f(\xi,t)=e^{-\xi^2}/\rho(t)$ vs x for the time (a) $(\omega_x)t=0$, (b) $(\omega_x)t=\pi/2$, and (c) $(\omega_x)t=\pi$. The space-time coordinates are normalized in units l_x and ω_x^{-1}, respectively.

$$|\psi(x,t)|^2 = \left| \sum_{n=0}^{\infty} C_n(t) R_n^{(0)}(\xi,t) e^{-in\theta(t)} \right|^2. \qquad (22)$$

In spite of the formula (22) with Eqs. (13) and (8) being complicated, some of its important features can be analyzed. After inserting Eq. (13) into Eq. (22) we find that there exists a common factor $f(\xi,t)=e^{-\xi^2}/\rho(t)$ in each term of Eq. (22). The function $\rho(t)$ included in $\xi=\sqrt{c_0}x/\rho(t)-b_0\sqrt{c_0^{-1}}\cos\theta(t)$ specifies the total width of the wave-packet train (22) and the width of each wave packet. The average width of the wave packets is $\rho(t)/\sqrt{c_0}$. The same function in the denominator of $f(\xi,t)$ governs the height of every wave packet. These and Eq. (8) infer that the widths and heights vary simultaneously with frequency $2\omega_x$ of the $\rho(t)$. Note that Eq. (14) gives the frequency of the center motion of the soliton train as ω_x. When the changes of the widths and heights are small, the behavior of the wave-packet trains seem to be an array of solitons. And larger changes of the widths and heights can show the periodical breathing behavior of the wave-packet trains [12,20], like the multiple breathers. The normalization condition implies that the broader wave-packet train is associated with the smaller mean height, and the narrower wave-packet train corresponds to the larger mean height. By using the parameter set $A=c_0=0.4624$, $B=1$, $\alpha=0$, $\beta=-\pi/2$, $b_0=-17.437$, we plot the function $f(\xi,t)=e^{-\xi^2}/\rho(t)$ vs x for the time $(\omega_x)t=0$, $\pi/2$, and π, respectively, as Figs. 1(a)–1(c). In Fig. 1 we show that a single wave packet varies its width and height periodically with period π and oscillates its center simultaneously with period 2π. These properties will directly affect the propagation and breathing of the soliton trains dominated by Eq. (22), since the function $f(\xi,t)$ appears in Eq. (22) as a factor. It is easy to prove the similar property for a different parameter set.

Although Eq. (20) is hard to solve in general, we can simplify it at the particular case: $\rho=\text{const}$. This implies $A=B$ and $\beta=\alpha-\pi/2$ in Eq. (8) such that we have $\rho=A$ and $\theta=t+\alpha$. Thus we can take $C_n(t)=D_n e^{in\theta}$ and substitute it and Eq. (13) into Eq. (20), obtaining the algebraical equations

$$-nD_n = g_{1d}\sum_{ijk}\left[D_i^* D_j D_k \int_{-\infty}^{\infty} R_i^{*(0)} R_j^{(0)} R_k^{(0)} R_n^{*(0)} dx \right] \qquad (23)$$

for $n=0,1,2,\ldots$, which determines the values of the constant coefficients D_n. Solving Eq. (23) for the D_n and applying Eq. (13) and $C_n(t)=D_n e^{in\theta}$ to Eq. (22), we get the density of atomic number,

$$|\psi(x,t)|^2 = \left| \sum_{n=0}^{\infty} D_n R_n^{(0)}(\xi,t) \right|^2. \qquad (24)$$

Here by the constant ρ we mean that Eq. (24) represents a real soliton train without any deformation.

We are interested in the case of time-dependent $\rho(t)$, where the Strecker's soliton trains with small deformation can be more exactly fit by Eq. (22). To solve Eq. (20) in this case, we must know its initial conditions. In Strecker's experiments, the end caps were switched off just at the initial time $t_0=0$ and the condensate was initially created on the side of the harmonic potential. The s-wave scattering length a_s changes sign at $t_1=t_0=0$, $t_2=35$ ms, …, respectively. In the first case $a_s|_{t_0}=0$, the two-body interaction term vanishes initially. The second case, $a_s|_{t_0}$ tending to zero, leads the initial soliton number to about 10. The small a_s means that the interaction term in Eq. (1) is much less than the harmonic term initially. This relation can be kept, since a_s vanishes at $t_2=35$ ms and after this time a_s is still a small value, $-3a_0$, with a_0 being the Bohr radius. Particularly, most of the condensed atoms are lost for $t>t_2$, while only a small fraction remains as solitons [1]. For the considered initial condition we integrate Eq. (20) producing

$$C_n(t) = \delta_{nn'} - ig_{1d}\int_0^t \sum_{ijk} I_{ijk}^n(t) C_i^*(t) C_j(t) C_k(t) dt. \qquad (25)$$

This gives $C_{n'}(0)=1$ and $C_n(0)=0$ for $n\neq n'$. Inserting these into Eq. (22) gives the initial wave packets in the form of $|\psi_{n'}^{(0)}|^2$ with the wave-packet number $n'+1$. This initial number can be fixed by Strecker's experimental data. Application of Eq. (25) to Eq. (22) leads to the soliton train at any time $t\geqslant 0$.

Because of the complexity of the solution behavior, numerically illustrating the soliton train is necessary. Generally, the wave-packet trains dominated by Eq. (22) will propagate and breathe simultaneously. We shall demonstrate that these complicated behaviors can be strictly fit to Strecker's matter-wave soliton trains. In the experiment reported by Strecker and co-workers [1], the ^{7}Li atomic BEC is employed to create the soliton trains, by using a Feshbach resonance to manipulate the sign and magnitude of the s-wave scattering length a_s. It is especially interesting to investigate the formation of the soliton trains. Setting Δt as the interval between the time the end caps of Strecker's experiment are switched off to the time when a_s changes sign, Strecker *et al.* found that the initial number of the solitons increases linearly with Δt. At $\Delta t=0$, namely the case that the end caps are switched off at $a_s \approx 0$, four solitons were observed initially [1]. The initial soliton number $n'+1$ means that a larger quantum number n' is associated with more solitons. This initial number may be greater than 10 in Strecker's experiment for the ^{7}Li atoms. Here the atomic number to form solitons is about $N=10^4$ and the oscillating frequency and amplitude of the center of soliton trains were experimentally observed, about 20 Hz (namely period $T\approx 310$ ms) and 370 μm, respectively. This frequency was identified as the axial one, ω_x, in the previous analytical work [6]. Note that the axial potential is approximately harmonic with angular frequency $\omega_x \sim 4 \times 2\pi$ Hz in Strecker's analysis [1]. We adopt the experimental parameter, $\omega_x=20$ Hz, rather than the analytically approximate one. From Fig. 4 of Ref. [1] we estimate that the maximum and minimum widths of the soliton trains are about 310 and 140 μm. Noticing the center oscillation amplitude Ab_0/c_0 in Eq. (14) and the average width of the wave packets $\rho(t)/\sqrt{c_0}$, these experimental data give rough limitations to the parameters in Eqs. (22) and (13) as $N=10^4$, $\omega_x=20$ Hz, $\omega_r=800$ Hz, $l_x=\sqrt{40}l_r=21.22$ μm, $Ab_0/c_0=-17.437l_x=-370$ μm, $\rho(0)/\sqrt{c_0}=6.8l_x\approx 140$ μm, $\rho(\pi/2)/\sqrt{c_0}=14.71l_x\approx 310$ μm. Under these limitations, we choose the parameter set $n'=10$, $a_s=-3a_0$, $A=c_0=0.4624$, $B=1$, $\alpha=0$, $\beta=-\pi/2$, $b_0=-17.437$, and the transverse wave function as the ground state of harmonic oscillator to make the 3D plots of the soliton train from Eqs. (22) and (25) for the time $(\omega_x)t=0$, $\pi/2$ and π, respectively, as Figs. 2(a)–2(c). Here the small terms being proportional to $C_n(t)$ for $n>20$ have been neglected in the series of Eq. (22). In Figs. 2(a) and 2(c) we show that the center-of-mass coordinates of the soliton train are $x_c(t=0)=-17.437l_x=-370$ μm and $x_c(t=T/2)=17.437l_x=370$ μm, respectively at $(\omega_x)t=0$ and π. These plots display that the soliton train localized at two ends of the trap possesses the maximum height and the minimum width and distance between two packets. When it moves to center of the trap, as in Fig. 2(b), its width and the distance between two packets become maximum, and its height reaches a minimum. The deformation period of the soliton train and the oscillation period of its center are π/ω_x and $2\pi/\omega_x$, respectively. In the next deformation period $\pi \leqslant \omega_x t \leqslant 2\pi$, the soliton train will propagate from right to left of the trap and go back to the initial place. These data and properties are in good agreement with that of Strecker's experiment.

The changes of the soliton width and distance between two solitons were explained as repulsive interaction among the solitons in the previous work [1,6]. In the motion of the soliton train, its height has only a small change such that observing the breathing effect is difficult. The solitons at ends of any soliton train are higher and thicker compared to the other ones. The thickness of each soliton is shown in Fig. 3, which denotes the vertical view of Fig. 2. This graph is very much like Fig. 4 of Strecker's article [1], so the former could be a good fit to the latter. In Strecker's experiment on the matter-wave solitons, the trains with missing solitons were frequently observed, and this is resided in the loss of condensed atoms [1] and the dissipative three-body interaction [5].

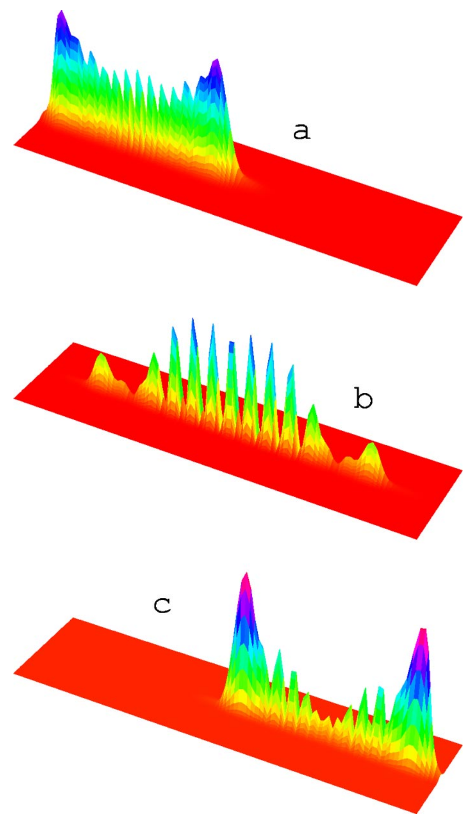

FIG. 2. (Color online) The Strecker's matter-wave solition trains on the xoy plane from Eqs. (22) and (13) for (a) $t=0$, (b) $\omega_x t=\pi/2$, and (c) $\omega_x t=\pi$. The transverse wave function has been taken as the ground state of harmonic oscillator. The space-time coordinates and the atomic number density $|\psi|^2$ are normalized in units l_x, ω_x^{-1}, and l_x^{-3}, respectively.

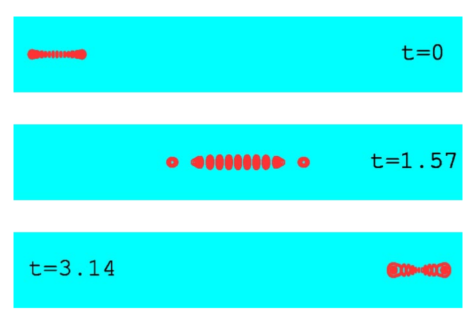

FIG. 3. (Color online) The vertical view of Fig. 2 with different lines correspond to Figs. 2(a)–2(c), respectively. Comparison between this with Fig. 4 of Strecker's article exhibits good agreement between them.

IV. DISCUSSION AND CONCLUSIONS

We have investigated the general case of soliton solution (18) with Eq. (13), where $b_0 \neq 0$ and $\rho(t)$ is a periodical function without zero point. When the amplitude of $\rho(t)$ is small, the wave-packet train described by Eq. (22) has only small deformation and seems to be a soliton train. By selecting a suitable parameter set, the solution fits the Strecker's soliton train better. A larger amplitude of $\rho(t)$ will lead Eq. (22) to describe the breathing behavior of the atomic number density. It is very interesting to see the special cases: (i) $b_0 = 0$; (ii) $\rho = \text{const}$; (iii) $\rho(t)$ has infinite zero points. Obviously, Eq. (14) gives $x_c = 0$ for $b_0 = 0$ such that the center of the wave-packet train described by Eqs. (22) and (13) cannot propagate for this case. We have demonstrated that the function $\rho(t)$ governs the widths and heights of the wave-packet trains, and the distance between two solitons. When the parameter set $A = B$, $\beta = \alpha - \pi/2$ is selected, Eq. (8) leads ρ to a constant and θ to the linear function $\omega_x t + \alpha$. Consequently, the wave-packet trains have not any deformation in propagation for the second case, which is described by Eq. (24). In this case, the ground state of Eq. (13) with $n = 0$ is just the common coherent state of a harmonic oscillator [13]. Setting $B = 0$ in Eq. (8) yields the third case, $\rho(t) = A\cos(\omega_x t + \alpha)$ with the infinite zero points $\omega_x t = (l + 1/2)\pi - \alpha$ for $l = 0, 1, 2, \ldots$. At any one of the zero points, Eq. (13) implies $\psi_n^{(0)} = \infty$ for $x \approx 0$, resulting in the intermittent implosions of the BEC [22,14].

Because of the existence of arbitrary constants A, B, α, β, b_0, c_0 and periodic functions $\rho(t)$, $\theta(t)$ in Eq. (13), by using the series solution (18) and adjusting these constants we can control the motions of the BEC wave packets. The theoretical control could indicate the directions of the experimental operations that is important for a real application, say, making an atomic soliton laser based on the bright soliton trains [1]. In addition, as a basic vector of Hilbert space the complete solution (13) could play an important role for treating the corresponding quantum systems.

ACKNOWLEDGMENTS

This work was supported by the National Natural Science Foundation of China under Grant No. 10275023, and by the foundations of MPI-PKS. The authors thank Dr. J. Brand for useful discussions.

[1] K. E. Strecker, G. B. Partridge, A. G. Truscott, and R. G. Hulet, Nature (London) **417**, 150 (2002).
[2] L. Khaykovich, F. Schreck, G. Ferrari, T. Bourdel, J. Cubizolles, L. D. Carr, Y. Castin, and C. Salomon, Science **296**, 1290 (2002).
[3] J. Denschlag, J. E. Simsarian, D. L. Feder, Charles W. Clark, L. A. Collins, J. Cubizolles, L. Deng, E. W. Hagley, K. Helmerson, W. P. Reinhardt, S. L. Rolston, B. I. Schneider, and W. D. Phillips, Science **287**, 97 (2000).
[4] L. D. Carr and J. Brand, Phys. Rev. Lett. **92**, 040401 (2004).
[5] L. Salasnich, A. Parola, and L. Reatto, Phys. Rev. Lett. **91**, 080405 (2003).
[6] U. Al Khawaja, H. T. C. Stoof, R. G. Hulet, K. E. Strecker, and G. B. Partridge, Phys. Rev. Lett. **89**, 200404 (2002).
[7] G. Chong, W. Hai, and Q. Xie, Chin. Phys. Lett. **20**, 2098 (2003).
[8] N. G. Parker, N. P. Proukakis, M. Leadbeater, and C. S. Adams, Phys. Rev. Lett. **90**, 220401 (2003).
[9] A. V. Yulin, D. V. Skryabin, and P. St. J. Russel, Phys. Rev. Lett. **91**, 260402 (2003).
[10] Dimitri J. Frantzeskakis, G. Theocharis, F. K. Diakonos, Peter Schmelcher, and Yuri S. Kivshar, Phys. Rev. A **66**, 053608 (2002).
[11] G. Huang, J. Szeftel, and Shanhua Zhu, Phys. Rev. A **65**, 053605 (2002).
[12] W. Hai, S. Huang, and K. Gao, J. Phys. B **36**, 3055 (2003).
[13] J. R. Klauder and B. Skagerstam, *Coherent States* (World Scientific Press, Singapore, 1985).
[14] W. Hai, C. Lee, G. Chong, and L. Shi, Phys. Rev. E **66**, 026202 (2002).
[15] C. Lee, W. Hai, L. Shi, X. Zhu, and K. Gao, Phys. Rev. A **64**, 053604 (2001).
[16] G. Chong, W. Hai, and Q. Xie, Chaos **14**, 217 (2004).
[17] Q. Xie, W. Hai, and G. Chong, Chaos **13**, 801 (2003).
[18] F. Dalfovo, S. Giorgini, L. P. Pitaevskii, and S. Stringari, Rev. Mod. Phys. **71**, 463 (1999).
[19] S. A. Gardiner, D. Jaksch, R. Dum, J. I. Cirac, and P. Zoller, Phys. Rev. A **62**, 023612 (2000).
[20] M. M. Nieto and D. R. Truax, New J. Phys. **2**, 18 (2000); Phys. Rev. Lett. **71**, 2843 (1993).
[21] Q. Thommen, J. C. Garreau, and V. Zehnle, Phys. Rev. Lett. **91**, 210405 (2003).
[22] H. Saito and M. Ueda, Phys. Rev. Lett. **86**, 1406 (2001).